Environmental Science & Technology

Caltech Library

Subscriber access provided by Caltech Library

Anthropogenic Impacts on the Atmosphere

Synthesis of Carboxylic Acid and Dimer Ester Surrogates to Constrain the Abundance and Distribution of Molecular Products in #-Pinene and #-Pinene Secondary Organic Aerosol

Christopher M Kenseth, Nicholas J. Hafeman, Yuanlong Huang, Nathan F. Dalleska, Brian M. Stoltz, and John H. Seinfeld

Environ. Sci. Technol., **Just Accepted Manuscript** • DOI: 10.1021/acs.est.0c01566 • Publication Date (Web): 19 Aug 2020

Synthesis of Carboxylic Acid and Dimer Ester Surrogates to Constrain the Abundance and Distribution of Molecular Products in α-Pinene and β-Pinene Secondary Organic Aerosol

Christopher M. Kenseth, Nicholas J. Hafeman, Yuanlong Huang,
Nathan F. Dalleska, Brian M. Stoltz, and John H. Seinfeld*

ABSTRACT: Liquid chromatography/negative electrospray ionization mass spectrometry [LC/(−)ESI-MS] is routinely employed to characterize the identity and abundance of molecular products in secondary organic aerosol (SOA) derived from monoterpene oxidation. Due to a lack of authentic standards, however, commercial terpenoic acids (e.g., *cis*-pinonic acid) are typically used as surrogates to quantify both monomeric and dimeric SOA constituents. Here, we synthesize a series of enantiopure, pinene-derived carboxylic acid and dimer ester homologues. We find that the (−)ESI efficiencies of the dimer esters are 19–36 times higher than that of *cis*-pinonic acid, demonstrating that the mass contribution of dimers to monoterpene SOA has been significantly overestimated in past studies. Using the measured (−)ESI efficiencies of the carboxylic acids and dimer esters as more representative surrogates, we determine that molecular products measureable by LC/(−)ESI-MS account for only 21.8 ± 2.6% and 18.9 ± 3.2% of the mass of SOA formed from ozonolysis of α-pinene and β-pinene, respectively. The 28–36 identified monomers ($C_{7–10}H_{10–18}O_{3–6}$) constitute 15.6–20.5% of total SOA mass, whereas only 1.3–3.3% of the SOA mass is attributable to the 46–62 identified dimers ($C_{15–19}H_{24–32}O_{4–11}$). The distribution of identified α-pinene and β-pinene SOA molecular products is examined as a function of carbon number (n_C), average carbon oxidation state ($\overline{OS}_C$), and volatility (C*). The observed order-of-magnitude difference in (−)ESI efficiency between monomers and dimers is expected to be broadly applicable to other biogenic and anthropogenic SOA systems analyzed via (−) or (+) LC/ESI-MS under various LC conditions, and demonstrates that the use of unrepresentative surrogates can lead to substantial systematic errors in quantitative LC/ESI-MS analyses of SOA.

INTRODUCTION

Secondary organic aerosol (SOA) comprises a substantial mass fraction (15–80%) of atmospheric fine particulate matter ($PM_{2.5}$),[1] and plays a pivotal role in climate,[2] air quality, and health.[3,4] Monoterpenes ($C_{10}H_{16}$), emitted in large quantities from terrestrial vegetation (~150 Tg y^{-1}),[5] represent a dominant source of SOA globally.[6–9] Deciphering the molecular composition, and in turn formation mechanisms, of monoterpene SOA is essential to reducing uncertainty in assessment of its environmental and health impacts. However, molecular characterization of monoterpene SOA is significantly hindered by its chemical complexity.[10]

Electrospray ionization mass spectrometry (ESI-MS), typically coupled with liquid chromatographic (LC) separation, is among the most widely used analytical techniques for identification and quantification of SOA molecular constituents.[10,11] Multifunctional carboxylic acids and dimer esters have been identified via ESI-MS methods as significant components of both laboratory-derived[12–37] and ambient[16–18,24,26,27,29,38] monoterpene SOA, reportedly accounting for as much as 58% of chamber-generated SOA mass from α-pinene ozonolysis.[31] Due to a lack of authentic standards, the abundances of molecular products in monoterpene SOA are (*i*) represented as (mass-weighted) fractions of the total ion signal/chromatographic peak area[20–22,37] or (*ii*) quantified using commercially available terpenoic acids (e.g., *cis*-pinonic acid) as surrogates.[23,25,27–33] However, given the strong dependence of ESI efficiency on molecular structure,[39–42] these approaches could lead to inaccurate apportionment of monoterpene SOA mass.

In this work, we synthesize a series of enantiopure, pinene-derived carboxylic acid and dimer ester homologues to determine the effect of molecular size and functionality on the ESI efficiency of monoterpene SOA constituents. Using the measured ESI efficiencies of the carboxylic acids and dimer esters as more representative proxies for those of like-structured monomers and dimers, respectively, we quantify the abundances of the most extensive suite of molecular products identified to date in SOA derived from ozonolysis of α-pinene and β-pinene, which together account for over 50% of global monoterpene emissions.[5]

EXPERIMENTAL

Synthesis of Carboxylic Acids and Dimer Esters. (+)-*cis*-Pinonic acid (**1**), (+)-*cis*-pinic acid (**2**), and (+)-*cis*-pinolic acid (**3**) were prepared according to modified literature procedures[43,44] from commercial (+)-α-pinene (98%, 89% ee, Sigma-Aldrich) in 56–88% yield (Scheme 1). Dimer esters **4–6** were synthesized as single stereoisomers in 38–59% yield from alcohol **3a** via Steglich esterification followed by Pd/C-catalyzed hydrogenolysis (Scheme 1). Experimental procedures, characterization data, and NMR and IR spectra for carboxylic acids **1–3,** dimer esters **4–6**, and all synthetic intermediates are provided in the Supporting Information (SI).

SOA Formation Experiments. α-Pinene and β-pinene ozonolysis experiments were carried out in the Caltech dual 24 m^3 Teflon Environmental Chambers (CTEC).[45] Experimental conditions are reported in Table 1 and time series of reactants/products for a representative experiment are shown in Figure S1. Prior to each experiment, the chamber was flushed with dry, purified air for 24 h such that the particle number and volume concentrations were less than 10 cm^{-3} and 0.01 μm^3 cm^{-3}, respectively. α-Pinene or β-pinene (~100 ppb) was added to the chamber by passing dry, purified air through a glass cylinder, warmed to 50 °C with electrical heat tape, containing a volumetric injection (15.5 μL) of liquid (+)-α-pinene (≥99%, Sigma-Aldrich) or (–)-β-pinene (≥99%, Sigma-Aldrich). Polydisperse seed aerosol (~90–280 μm^3 cm^{-3}, $\overline{D}_p \approx 144 \pm 17$ nm) was generated via atomization of a dilute (0.06 M) aqueous solution of $(NH_4)_2SO_4$ (Macron Fine Chemicals), followed by diffusive drying and neutralization. O_3 (~150 ppb) was produced by flowing dry, purified air through a custom-built UV O_3 generator. Ozonolysis experiments were conducted in the absence of an OH scavenger, resulting in initial OH molar yields for α-pinene and β-pinene of 77–89%[46,47] and 28–44%,[48,49] respectively. Under these conditions, ~97% of α-pinene and ~58% of β-pinene was consumed over ~5 h of reaction in the CTEC.

Gas-Phase Instrumentation. α-Pinene and β-pinene mixing ratios were quantified with an Agilent 6890N gas chromatograph equipped with a flame ionization detector (GC/FID) and operated with an Agilent HP-5 column (30 m × 0.32 mm, 0.25 μm). The GC/FID was calibrated as described in Kenseth et al.[34] α-Pinene and β-pinene decay curves over ~5 h of ozonolysis in the CTEC are shown in Figure 1A. O_3 and NO_x mixing ratios were quantified by a Horiba APOA-360

O_3 monitor and a Teledyne T200 NO_x analyzer, respectively. Temperature and relative humidity (RH) were monitored with a Vaisala HMM211 probe.

Particle-Phase Instrumentation. *Scanning Mobility Particle Sizer (SMPS).* Aerosol size distributions and number concentrations ($D_p \approx 15–800$ nm) were measured with a custom-built SMPS consisting of a TSI 3081 differential mobility analyzer (DMA) coupled to a TSI 3010 condensation particle counter (CPC). Details of the SMPS operation are provided elsewhere.[34,50] Suspended SOA volume concentrations were derived using the approach of Kenseth et al.,[34] and were not corrected for particle wall loss to enable direct comparison with the concentrations of individual molecular products detected in suspended SOA using off-line mass spectrometry. SOA mass concentrations were calculated assuming an effective density of 1.25 g mL^{-1} for α-pinene and β-pinene SOA.[51–54] Growth profiles of suspended SOA produced from ozonolysis of α-pinene and β-pinene over ~5 h of reaction in the CTEC are shown in Figure 1B.

High-Resolution Time-of-Flight Aerosol Mass Spectrometer (HR-ToF-AMS). Submicrometer, nonrefractory aerosol chemical composition was quantified with an Aerodyne HR-ToF-AMS[55] configured in V-mode. Detection limits and instrumental ionization efficiencies for each class of speciated constituents (i.e., sulfate, ammonium, and organics) were determined following the methods in Kenseth et al.[34] Data were analyzed using the SQUIRREL v1.61 and PIKA v1.21 modules for Igor Pro v7.08 (WaveMetrics), and were corrected for gas-phase interferences[56,57] and composition-dependent collection efficiencies.[58] Elemental O:C and H:C ratios, as well as average carbon oxidation states ($\overline{OS}_C$ = 2 O:C − H:C), were calculated using the "Improved-Ambient" elemental analysis method for AMS spectra.[59] Average O:C and $\overline{OS}_C$ values for α-pinene and β-pinene SOA after ~5 h of ozonolysis in the CTEC are reported in Table 1. These values are in good agreement with O:C and H:C ratios previously reported for laboratory-derived SOA formed from α-pinene ozonolysis (O:C = 0.30–0.43; H:C = 1.47–1.66).[30,59–63]

Particle-Into-Liquid Sampler (PILS). A custom-modified PILS was used to collect chamber-generated α-pinene and β-pinene SOA for off-line, molecular-level characterization. A detailed description of the Caltech PILS is presented elsewhere.[34,64] Briefly, sampled aerosol (1-μm cut size, 12.5 L min^{-1} flow rate) is passed through successive acid, base, and organic carbon denuders

into a condensation chamber where particles grow sufficiently large (D_p > 1 μm) for collection by inertial impaction via adiabatic mixing with steam generated from ultra-pure water (18.2 MΩ cm, <3 ppb TOC, Millipore Milli-Q). Impacted particles are transported to a debubbler by a washing flow (0.15 mL min^{-1}) of ultra-pure water, and the sampled liquid is delivered into vials (5-min duty cycle) held on a rotating carousel. Sample vials were stored at −16 °C immediately after collection. The overall PILS collection efficiency for α-pinene and β-pinene SOA was estimated to be >85%, based on an empirical correlation of water solubility and the AMS-derived bulk O:C ratio of the SOA.[65]

Ultra-Performance Liquid Chromatography/Negative Electrospray Ionization Quadrupole Time-of-Flight Mass Spectrometry [UPLC/(–)ESI-Q-TOF-MS]. α-Pinene and β-pinene SOA PILS samples were analyzed by a Waters ACQUITY UPLC I-Class system coupled to a Xevo G2-S Q-TOF-MS equipped with an ESI source and operated in (–) ion mode. An ACQUITY BEH C_{18} column (1.7 μm, 2.1 mm × 50 mm) fitted with an ACQUITY BEH C_{18} VanGaurd pre-column (1.7 μm, 2.1 mm × 5 mm) was used to separate SOA molecular constituents. Instrument specifications, acquisition parameters (e.g., gradient-elution and MS/MS methods), and calibration procedures are detailed in Kenseth et al.[34] Note that due to the addition of the guard column, retention times (t_R) of SOA molecular products are shifted by +0.11–0.15 min compared to those reported in Kenseth et al.[34] All analytes were detected as $[M–H]^-$ ions, generated via deprotonation of parent molecules during (–)ESI. Instrument stability (i.e., chromatographic and mass spectral reproducibility) was verified to within 4% using an equimolar (1.00 μM) aqueous solution of carboxylic acids **1–3** and dimer esters **4–6**, run twice every 10 samples during routine analysis. Data were acquired and processed using MassLynx v4.1 software. Molecular formulas ($C_xH_yO_z$) of $[M–H]^-$ ions were assigned with mass tolerances of <7 ppm and supported by the associated ^{13}C isotope distributions.

Quantification of SOA Molecular Products. Mass concentrations of individual organic compounds in chamber-generated α-pinene and β-pinene SOA collected by PILS and analyzed off-line by UPLC/(–)ESI-Q-TOF-MS were calculated from the following expression:

$$C = \frac{Q_l \cdot DF \cdot R \cdot M}{Q_s \cdot CE_{PILS} \cdot IE} \quad (1)$$

where C is the particle-phase mass concentration of the compound (μg m^{-3}), Q_s is the aerosol sampling flow rate (12.5 L min^{-1}), Q_l is the rate of the washing flow (0.15 mL min^{-1}), DF is the dilution factor that accounts for water vapor condensation on the PILS impaction plate (assumed to be 1.1),[64] CE_{PILS} is the overall PILS collection efficiency for α-pinene and β-pinene SOA (estimated to be 0.85),[65] R is the UPLC/(–)ESI-Q-TOF-MS response for the compound [i.e., extracted ion chromatogram (EIC) peak area], M is the molecular weight of the compound (g mol^{-1}), and IE is the compound-specific (–)ESI efficiency (μM^{-1}). Prior separation of analytes from the complex SOA matrix via UPLC precludes potential ion-source artifacts (e.g., signal suppression and noncovalent clustering), ensuring the quantitative nature of the method. From comparison of the resulting particle-phase mass concentrations to the SMPS-derived suspended SOA mass loading, mass fractions of identified molecular products in α-pinene and β-pinene SOA were determined.

Due to a lack of authentic standards, (–)ESI efficiencies of monomers and dimers identified in α-pinene and β-pinene SOA were quantified using those measured for carboxylic acids **1–3** and dimer esters **4–6** as surrogates. Weighted (1/X), linear ($R^2 > 0.998$) calibration curves were generated from triplicate measurements of equimolar aqueous solutions of carboxylic acids **1–3** and dimer esters **4–6** spanning a concentration range from 0.200 to 5.00 μM (Figure 2); all surrogates were fully water soluble at 5.00 μM (295 K, 1 atm). Limits of quantitation (LOQ), calculated as ten times the standard deviation of the blank ($10\sigma_{blank}$), were found to range from 1.8–2.7 nM for dimer esters **4–6** to 8.1–39 nM for carboxylic acids **1–3** and are reported in Table S2, along with limits of detection (LOD, $3\sigma_{blank}$) and (–)ESI efficiencies (μM^{-1}). The concentration of every monomer and dimer measured in the PILS samples fell above the LOQ and within the calibrated linear range of the corresponding surrogate.

Uncertainty Analysis. Uncertainty in the PILS method (δ_{PILS}) arises mainly from variation in the collected liquid volume due to imperfect debubbling, and has been estimated to be less than ±11%.[65] Uncertainty associated with the chromatographic and mass spectral reproducibility of the

UPLC/(–)ESI-Q-TOF-MS (δ_{UPLC}) was determined to be less than ±4% (see above). Uncertainty in the concentrations of the calibration standards for carboxylic acids **1–3** and dimer esters **4–6** due to the precision of the analytical balance and Class A volumetric glassware (δ_{CalStd}) was calculated to be less than ±1%. Uncertainty in the measured (–)ESI efficiencies of carboxylic acids **1–3** and dimer esters **4–6** ($\delta_{(-)ESI}$) was found to be less than ±1%. An uncertainty of ±20% is assumed for SMPS-derived suspended SOA mass loadings (δ_{SMPS}).[66] Propagation of these individual uncertainties yields a total estimated relative uncertainty in the reported SOA mass fractions (δ_{total}) of ±23%:

$$\delta_{\text{total}} = \sqrt{\delta_{\text{PILS}}^2 + \delta_{\text{UPLC}}^2 + \delta_{\text{CalStd}}^2 + \delta_{(-)\text{ESI}}^2 + \delta_{\text{SMPS}}^2} = 0.23 \quad (2)$$

Note, however, that this method uncertainty is not explicitly quoted in the following sections. Rather, all data are reported as averages of replicate experiments for α-pinene ($n = 4$) and β-pinene ($n = 5$) together with their standard deviations (1σ).

RESULTS AND DISCUSSION

(–)ESI Efficiencies of Carboxylic Acids and Dimer Esters. Equimolar aqueous solutions of carboxylic acids **1–3** and dimer esters **4–6** were analyzed by UPLC/(–)ESI-Q-TOF-MS; a representative base peak ion (BPI) chromatogram and weighted (1/X) calibration curves are shown in Figure 2. Contrary to the assumptions of previous LC/(–)ESI-MS studies that monoterpene oxidation products exhibit comparable (–)ESI efficiencies due to the presence of similar structures/functional groups,[20–22] the (–)ESI efficiencies of carboxylic acids **1–3** varied by almost a factor of six despite differing only in the identity of the terminal functional group (i.e., ketone vs. carboxylic acid vs. alcohol). More strikingly, the (–)ESI efficiencies of dimer esters **4–6** were found to be 19–36 times higher than that of commercially available *cis*-pinonic acid (**1**). These findings conclusively demonstrate that as a result of fundamental differences in ionizing behavior, the mass contribution of dimers (and to a lesser extent dicarboxylic acids) to monoterpene SOA has been significantly overestimated in past studies.[20–23,25,27–33]

The observed trends in (–)ESI efficiency for carboxylic acids **1–3** and dimer esters **4–6** are consistent with the current understanding of the (–)ESI process, which for molecules <1000 Da is

described by the ion evaporation model (IEM).[39] To first order, (–)ESI efficiency depends on (*i*) the degree of ionization in solution, a function of analyte acidity (pK_a) and the number of potentially ionizable (carboxyl) groups, and (*ii*) the ease of ion evaporation from the ESI droplet, which relates to the extent of ion charge delocalization and increases with molecular size (i.e., larger molecules produce ions with more delocalized charge).[41,42] Mechanistically, compounds that are more extensively dissociated in solution will yield a higher concentration of anions in ESI droplets, while anions with more delocalized charge will more readily partition to and evaporate from ESI droplet surfaces due to lower solvation energy and a lower tendency for ion pairing (i.e., weaker interaction with solvent molecules and cations in the droplet interior).[41] For LC/(–)ESI-MS analysis of SOA molecular constituents, therefore, (–)ESI efficiencies will scale with pK_a [$(-)ESI_{strong\_acid} > (-)ESI_{weak\_acid}$], the number of sites available for deprotonation [$(-)ESI_{diacid} \gtrsim 2(-)ESI_{monoacid}$], and (most strongly) molecular weight [$(-)ESI_{dimer} \gtrsim 10(-)ESI_{monomer}$]. Notably, the (–)ESI efficiencies estimated in our recent study for dimer esters in β-pinene SOA[34] by adapting the linear model of Kruve et al.,[41] which contains only the degree of solution ionization and anion charge delocalization as input parameters, effectively captured the order-of-magnitude difference in (–)ESI efficiency between monomers and dimers.

In addition to analyte properties, (–)ESI efficiency has been found to depend on the solvent composition of the ESI droplet.[42] Given the varying acetonitrile-water content of the gradient UPLC method (12–62% acetonitrile over t_R 3.00–7.50 min), the influence of eluent composition on the (–)ESI efficiencies of carboxylic acids **1–3** and dimer esters **4–6** was evaluated for an equimolar (1.00 μM) aqueous solution via isocratic UPLC/(–)ESI-Q-TOF-MS across a range of acetonitrile volume fractions (10–60%) (Figure S2). Compared to those obtained with the gradient method, the (–)ESI efficiencies of carboxylic acids **1–3** and dimer esters **4–6** changed by only 20–50% over the respective ranges of acetonitrile content within which monomers (10–30%) and dimers (40–60%) in α-pinene and β-pinene SOA elute during gradient UPLC. In contrast, the (–)ESI efficiencies of carboxylic acids **1–3** at 60% acetonitrile were found to be 1.6–1.9 times higher than those from the gradient method. As molecular structure determines the solvent composition at which an analyte elutes

from the LC column, the distinct (–)ESI behavior of monomers and dimers in LC/(–)ESI-MS, and the resultant overestimation of dimeric SOA mass fractions in past studies,[20,23,25,27–33] thus stems from both a direct (analyte properties) and lesser indirect (ESI droplet composition) dependence of (–)ESI efficiency on molecular structure.

Abundance of Molecular Products in α-Pinene and β-Pinene SOA. Replicate α-pinene (n = 4) and β-pinene (n = 5) ozonolysis experiments were carried out in the CTEC (Figure 1, Table 1). PILS + UPLC/(–)ESI-Q-TOF-MS was used to characterize the SOA molecular composition (5-min average) after ~5 h of reaction; representative BPI chromatograms are shown in Figure S3. A total of 36 monomers ($C_{7–10}H_{10–18}O_{3–6}$) and 46 dimers ($C_{15–19}H_{24–30}O_{4–10}$) were identified in α-pinene SOA, while 28 monomers ($C_{7–10}H_{10–18}O_{3–6}$) and 62 dimers ($C_{15–19}H_{24–32}O_{5–11}$) were identified in β-pinene SOA (Table S3). Many of these compounds are isomers that elute at unique t_R. The monomers, in general, exhibit higher O:C ratios (0.30–0.75) than the dimers (0.22–0.63), suggesting that deoxygenation (e.g., condensation) is involved in dimer formation.[12,14,34] That the dimers elute at t_R distinct from those of the monomers demonstrates that they are authentic, covalently bound SOA products and not ion-source artifacts formed during the (–)ESI process.

Using the measured (–)ESI efficiencies of carboxylic acids **1**–**3** and dimer esters **4**–**6** as surrogates for those of like-structured (i.e., mono vs. polycarboxylic) monomers and dimers, respectively (Table S3), identified molecular products were determined to account for 21.8 ± 2.6% and 18.9 ± 3.2% of α-pinene and β-pinene SOA mass, respectively. Notably, the dimers comprised only a small fraction (1.3–3.3%) of total SOA mass, whereas the mass contribution of the monomers was appreciable (15.6–20.5%) (Table 1). Based on comparison with authentic standards and/or previously reported LC/(–)ESI-MS data,[17,34] *cis*-pinic acid ($C_9H_{14}O_4$; t_R 4.45 min) and terpenylic acid ($C_8H_{12}O_4$; t_R 4.07 min) were identified as the most abundant monomers, with respective mass fractions of 3.9 ± 0.6% and 3.4 ± 0.6% in α-pinene SOA and 3.3 ± 0.6% and 3.3 ± 0.6% in β-pinene SOA. Similarly, pinyl-diaterpenyl ester ($C_{17}H_{26}O_8$; t_R 5.43 min) was found to be the most abundant dimer, constituting 0.2 ± 0.02% and 0.6 ± 0.1% of α-pinene and β-pinene SOA mass, respectively. Mass fractions and proposed molecular structures of the most abundant seven monomers and eight dimers identified in SOA from ozonolysis of α-pinene and β-pinene,

representing 13.8–15.5% of total SOA mass, are listed in Table S4, while mass fractions and physicochemical properties of all identified molecular products are presented in Table S3.

Comparison of the monomeric and dimeric SOA mass fractions derived in this work to those reported in two recent, comprehensive LC/(–)ESI-MS analyses of chamber-generated SOA from α-pinene ozonolysis[30,31] reveals significant discrepancies (Table 2). Encouragingly, however, adjustment of the mass fraction estimates in these studies based on the relative (–)ESI efficiencies of carboxylic acids **1**−**3** and dimer esters **4**−**6** (details provided in SI, Section S1) brings the three sets of mass fractions into general agreement and suggests that carboxyl-containing products constitute ~20–30% of the mass of chamber-generated SOA formed from α-pinene ozonolysis at 293–298 K and ~1 atm, under dry (<5% RH), low-NO_x (<1 ppb) conditions, and in the absence of an OH scavenger (Table 2). These findings are consistent with recent measurements of organic acids in laboratory-derived α-pinene SOA made with a filter inlet for gases and aerosol coupled to an acetate chemical ionization mass spectrometer (FIGAERO-CIMS).[67] Additionally, an average empirical relationship between the fraction of OA mass composed of organic acids (f_{acid}) and the fraction of AMS OA signal at *m/z* 44 (f_{44}) was recently developed based on acetate/O_2^- CIMS measurements of particle-phase organic acids and AMS data from three field campaigns in forested regions with significant monoterpene emissions [$f_{acid} = (2.50 \pm 0.19) f_{44}$].[68] Using the SOA mass fractions of total carboxyl-containing species detected by PILS + UPLC/(–)ESI-Q-TOF-MS and AMS data in this work, similar relationships were derived for chamber-generated SOA from ozonolysis of α-pinene [$f_{acid} = (2.54 \pm 0.22) f_{44}$] and β-pinene [$f_{acid} = (1.91 \pm 0.28) f_{44}$], further suggesting that a simple scaling of AMS f_{44} by a factor of ~2–2.5 can provide a reasonable estimate of the mass contribution of organic acids to OA with appreciable monoterpene SOA influence.

The use of carboxylic acids **1–3** and dimer esters **4–6** as surrogates to quantify the respective mass fractions of monomers and dimers identified in α-pinene and β-pinene SOA represents a significant analytical improvement compared to previous LC/(–)ESI-MS studies.[20–23,25,27–33] Due to the lack of structural information for the majority of identified carboxyl-containing species, however, and the dependence of (–)ESI efficiency on the number of ionizable carboxyl groups, the SOA mass fractions of monomers and dimers with unknown structures, respectively quantified

using carboxylic acid **1** and dimer ester **6** as defaults (Table S3), are likely overestimated for those that possess two or more carboxyl groups. Likewise, SOA mass fractions for molecular products with proposed structures containing three or more carboxyl groups [e.g., pinyl-diaterpenyl ester[17] and 3-methyl-1,2,3-butanetricarboxylic acid (MBTCA)[19]], calculated using carboxylic acid **2** or dimer ester **4** (Table S3), are expected to constitute overestimates. Together, these structural limitations imply that molecular products measureable by LC/(−)ESI-MS may account for an even smaller fraction of α-pinene and β-pinene SOA mass than reported here, particularly dimeric compounds given the dominant mass contribution of pinyl-diaterpenyl ester.

Distribution of Molecular Products in α-Pinene and β-Pinene SOA. Mass fractions of identified molecular products in SOA derived from ozonolysis of α-pinene and β-pinene are shown in Figure 3 as a function of carbon number (n_C). For $C_{7–9}$ compounds, as well as total monomers ($C_{7–10}$), statistically similar SOA mass fractions for α-pinene and β-pinene were obtained. Conversely, the fraction of SOA mass attributable to C_{10} species was considerably larger in the α-pinene system, in line with established gas-phase ozonolysis mechanisms (i.e., the carbon backbone of endocyclic α-pinene is retained on ozonolysis whereas the terminal vinylic carbon of exocyclic β-pinene is cleaved).[48,49,69]

With the exception of C_{19} compounds, identified dimers ($C_{15–18}$) accounted for significantly larger fractions of β-pinene SOA mass, resulting in roughly a three-fold difference in total dimeric mass fraction between SOA produced from ozonolysis of α-pinene (1.3 ± 0.1%) and β-pinene (3.3 ± 0.6%). In part, this difference is explained by the much higher suspended SOA mass loadings formed in the α-pinene system (Figure 1, Table 1), due to the faster rate at which ozonolysis proceeds for α-pinene ($k_{\alpha p + O_3} = 8.4 \times 10^{-17}$ cm^3 molecules^{-1} s^{-1}) as compared to β-pinene ($k_{\beta p + O_3} = 1.5 \times 10^{-17}$ cm^3 molecules^{-1} s^{-1}).[70] At higher SOA loadings, equilibrium partitioning of semivolatile monomers becomes an increasingly dominant source of SOA mass, minimizing the mass contribution of (extremely) low-volatility dimers, which provide the main SOA source at low loading via irreversible condensation.[31,71] Even so, based on mass yields of total dimers identified in α-pinene (0.48 ± 0.01%) and β-pinene (0.80 ± 0.04%) SOA after ~5 h of reaction ($m_{total\_dimer}/m_{pinene\_reacted}$), ozonolysis of β-pinene appears to be more efficient at producing dimeric

compounds measureable by PILS + UPLC/(–)ESI-Q-TOF-MS. However, the mechanisms underlying dimer formation in these systems remain unresolved.[34]

Physicochemical Properties of Molecular Products in α-Pinene and β-Pinene SOA. Shown in Figure 4 are the molecular products identified in α-pinene and β-pinene SOA mapped onto the average carbon oxidation state vs. carbon number ($\overline{OS}_C$-n_C) space, as well as in mass defect plots. Note that in these frameworks, isomers are represented collectively as single data points. In terms of saturation mass concentration (C*), monomers ($C_{7–10}$) are classified as intermediate-volatility (IVOC; $300 < C^* < 3 \times 10^6$ μg m^{-3}), semivolatile (SVOC; $0.3 < C^* < 300$ μg m^{-3}), or low-volatility organic compounds (LVOC; $3 \times 10^{-4} < C^* < 0.3$ μg m^{-3}), whereas all dimers ($C_{15–19}$) are designated as extremely low-volatility organic compounds (ELVOC; $C^* < 3 \times 10^{-4}$ μg m^{-3}).[72] The molecular formulas of a number of these compounds are common to both α-pinene and β-pinene SOA and can largely be grouped into homologous series of monomers ($C_8H_{12}O_{4–6}$, $C_8H_{14}O_{4–6}$, and $C_9H_{14}O_{3–5}$) and dimers ($C_{16}H_{26}O_{6–10}$, $C_{17}H_{26}O_{5–9}$, $C_{18}H_{28}O_{4–11}$, and $C_{19}H_{30}O_{5–10}$). Distinct homologous series for α-pinene ($C_{10}H_{14}O_{4–6}$, $C_{10}H_{16}O_{3–6}$, $C_{18}H_{26}O_{6–8}$, and $C_{19}H_{28}O_{5–9}$) and β-pinene ($C_{17}H_{28}O_{5–10}$ and $C_{18}H_{30}O_{6–10}$) were also observed.

The mass-weighted $\overline{OS}_C$ of the identified molecular products in α-pinene ($–0.62 \pm 0.07$) and β-pinene ($–0.57 \pm 0.10$) SOA are significantly higher than the corresponding AMS-derived bulk $\overline{OS}_C$ values (Figure 4, Table 1), indicating that the SOA mass undetected by PILS + UPLC/(–)ESI-Q-TOF-MS (~80%) is less oxygenated, on average, than the identified carboxyl-containing species. The comparatively reduced nature of the unidentified SOA mass implies that particle-phase chemistry involving the loss of oxygen, particularly from highly oxygenated organic molecules (HOMs)[73] that have been implicated as important contributors to monoterpene SOA,[71,74–76] is operative in modulating the $\overline{OS}_C$ of α-pinene and β-pinene SOA molecular constituents. For example, decomposition of multifunctional organic (hydro)peroxides (e.g., peroxyhemiacetals and diacyl peroxides) in biogenic SOA, on time scales of hours or less, has been demonstrated in a number of recent studies[35,77–80] and can lead to nonperoxide species (e.g., carboxylic acids, aldehydes, and esters) with decreased oxygen content.[31,81,82]

In addition, despite being routinely measured in the gas phase,[71,74,76,83,84] C_{20} compounds were not detected in SOA from α-pinene ozonolysis, consistent with several recent LC/(−)ESI-MS studies.[14,24–31,35] This implies that C_{20} dimers, likely formed via gas-phase self/cross-reactions of organic peroxy radicals ($RO_2 + RO_2 \rightarrow ROOR + O_2$), undergo chemical transformation/decomposition following condensation to the particle phase, as previously suggested.[13,31,71] The decomposition of ROOR is in line with results from our recently developed iodometry-assisted LC/(−)ESI-MS assay, which found that only one compound identified in SOA from α-pinene ozonolysis ($C_8H_{14}O_6$) contained (hydro)peroxide moieties.[35] That said, the lack of detection by LC/(−)ESI-MS could also indicate that C_{20} compounds formed from α-pinene ozonolysis simply do not contain carboxyl groups.

ATMOSPHERIC IMPLICATIONS

Due to the inherent chemical complexity of SOA and resultant lack of authentic standards required for calibration, quantification of SOA molecular products via LC/ESI-MS is subject to the use of surrogates and proceeds under the assumption that compounds with similar structures/functionalities exhibit comparable ESI efficiencies. For α-pinene and β-pinene SOA, this has led to extensive use of commercial terpenoic acids (e.g., *cis*-pinonic acid) as surrogates for quantifying both monomeric and dimeric SOA constituents. However, in establishing that the (−)ESI efficiencies of dimer esters **4–6** are at least an order of magnitude higher than those of carboxylic acids **1–3**, which in turn differ by almost a factor of six, this study demonstrates that the use of unrepresentative surrogates can lead to substantial, previously unrecognized systematic errors in quantitative LC/ESI-MS analyses of SOA, particularly with respect to quantification of high-molecular-weight compounds using low-molecular-weight proxies. Although specifically elucidated via LC/(−)ESI-MS of pinene-derived carboxylic acids and dimer esters, the observed order-of-magnitude difference in (−)ESI efficiency between monomers and dimers is consistent with the general mechanistic understanding of the ESI process and is expected to be equally applicable to other biogenic and anthropogenic SOA systems analyzed via either (−) or (+) LC/ESI-MS under various LC conditions (e.g., organic solvent content, buffer concentration, and pH).[42]

The failure of past LC/(–)ESI-MS studies to account for the distinct (–)ESI behavior of monomers and dimers, and the consequent overestimation of dimeric (and polycarboxylic) SOA mass fractions (Table 2), has led carboxyl-containing compounds to be regarded as dominant constituents of α-pinene and β-pinene SOA; a reasonable supposition given that the carboxyl moiety represents an approximate endpoint in carbon oxidation state and its incorporation leads to a ~1000-fold reduction in vapor pressure relative to the parent compound.[67] However, constrained by the (–)ESI efficiencies of carboxylic acids **1**−**3** and dimer esters **4**−**6**, the 82–90 carboxyl-containing compounds identified in this work (Table S3), as well as those in previous LC/(–)ESI-MS studies (Table 2), are found to account for only ~20–30% of the mass of chamber-generated SOA from ozonolysis of α-pinene or β-pinene. In particular, the 46–62 identified ELVOC dimers, although still expected to play a critical role in new particle formation and growth (i.e., at low SOA loading), are determined to make only a minor contribution (~1–3%) to total α-pinene and β-pinene SOA mass. A substantial fraction (~70–80%) of α-pinene and β-pinene SOA mass remains undetected by LC/(–)ESI-MS methods. Based on comparison of AMS-derived bulk $\overline{OS}_C$ and mass-weighted molecular $\overline{OS}_C$ values, this unspeciated mass appears to be less oxygenated, on average, than identified carboxyl-containing species. However, elucidation of the molecular composition of the outstanding SOA mass (i.e., carbon closure) will require the concerted application and proper calibration of mass spectrometric techniques sensitive to other compound classes.

ASSOCIATED CONTENT

Supporting Information

Adjustment of mass fractions in published LC/(–)ESI-MS studies of SOA from α-pinene ozonolysis; Tables S1–S4 and Figure S1–S3; synthetic procedures, characterization data, and NMR and IR spectra for carboxylic acids **1–3,** dimer esters **4–6**, and all synthetic intermediates.

AUTHOR INFORMATION

Corresponding Author

John H. Seinfeld – *Divisions of Chemistry and Chemical Engineering and Engineering and Applied Science, California Institute of Technology, Pasadena, CA 91125*; orcid.org/0000-0003-1344-4068; Email: seinfeld@caltech.edu

Authors

Christopher M. Kenseth – *Division of Chemistry and Chemical Engineering, California Institute of Technology, Pasadena, CA 91125*; orcid.org/0000-0003-3188-2336

Nicholas J. Hafeman – *Division of Chemistry and Chemical Engineering, California Institute of Technology, Pasadena, CA 91125*; orcid.org/0000-0001-7525-7597

Yuanlong Huang – *Division of Geological and Planetary Sciences, California Institute of Technology, Pasadena, CA 91125*; orcid.org/0000-0002-6726-8904

Nathan F. Dalleska – *Environmental Analysis Center, Division of Geological and Planetary Sciences, California Institute of Technology, Pasadena, CA 91125*; orcid.org/0000-0002-2059-1587

Brian M. Stoltz – *Division of Chemistry and Chemical Engineering, California Institute of Technology, Pasadena, CA 91125*; orcid.org/0000-0001-9837-1528

Author Contributions

C.M.K. designed research; C.M.K. and Y.H. performed research; C.M.K., N.J.H., and B.M.S. contributed new reagents; C.M.K., Y.H., and N.F.D. analyzed data; and C.M.K. and J.H.S. wrote the paper.

Notes

The authors declare no competing financial interest.

ACKNOWLEDGMENTS

We thank John Crounse and Paul Wennberg for useful discussions. UPLC/(−)ESI-Q-TOF-MS was performed in the Caltech Environmental Analysis Center (EAC). This work was supported by National Science Foundation Grants AGS-1523500, CHE-1800511, and CHE-1905340. The EAC is supported by the Linde Center and Beckman Institute at Caltech.

REFERENCES

(1) Jimenez, J. L.; Canagaratna, M. R.; Donahue, N. M.; Prevot, A. S. H.; Zhang, Q.; Kroll, J. H.; DeCarlo, P. F.; Allan, J. D.; Coe, H.; Ng, N. L.; Aiken, A. C.; Docherty, K. S.; Ulbrich, I. M.; Grieshop, A. P.; Robinson, A. L.; Duplissy, J.; Smith, J. D.; Wilson, K. R.; Lanz, V. A.; Hueglin, C.; Sun, Y. L.; Tian, J.; Laaksonen, A.; Raatikainen, T.; Rautiainen, J.; Vaattovaara, P.; Ehn, M.; Kulmala, M.; Tomlinson, J. M.; Collins, D. R.; Cubison, M. J.; E.; Dunlea, J.; Huffman, J. A.; Onasch, T. B.; Alfarra, M. R.; Williams, P. I.; Bower, K.; Kondo, Y.; Schneider, J.; Drewnick, F.; Borrmann, S.; Weimer, S.; Demerjian, K.; Salcedo, D.; Cottrell, L.; Griffin, R.; Takami, A.; Miyoshi, T.; Hatakeyama, S.; Shimono, A.; Sun, J. Y.; Zhang, Y. M.; Dzepina, K.; Kimmel, J. R.; Sueper, D.; Jayne, J. T.; Herndon, S. C.; Trimborn, A. M.; Williams, L. R.; Wood, E. C.; Middlebrook, A. M.; Kolb, C. E.; Baltensperger, U.; Worsnop, D. R. Evolution of Organic Aerosols in the Atmosphere. *Science* **2009**, *326* (5959), 1525–1529. https://doi.org/10.1126/science.1180353.

(2) Intergovernmental Panel on Climate Change. *Climate Change 2013: The Physical Science Basis*; Stocker, T. F., Qin, D., Plattner, G. K., Tignor, M., Allen, S. K., Boschung, J., Nauels, A., Xia, Y., Bex, V., Midgley, P. M., Eds.; Cambridge University Press: Cambridge, United Kingdom, 2013.

(3) Pope, C. A.; Ezzati, M.; Dockery, D. W. Fine-Particulate Air Pollution and Life Expectancy in the United States. *N. Engl. J. Med.* **2009**, *360* (4), 376–386. https://doi.org/10.1056/NEJMsa0805646.

(4) Cohen, A. J.; Brauer, M.; Burnett, R.; Anderson, H. R.; Frostad, J.; Estep, K.; Balakrishnan, K.; Brunekreef, B.; Dandona, L.; Dandona, R.; Feigin, V.; Freedman, G.; Hubbell, B.; Jobling, A.; Kan, H.; Knibbs, L.; Liu, Y.; Martin, R.; Morawska, L.; Pope, C. A.; Shin, H.; Straif, K.; Shaddick, G.; Thomas, M.; van Dingenen, R.; van Donkelaar, A.; Vos, T.; Murray, C. J. L.; Forouzanfar, M. H. Estimates and 25-Year Trends of the Global Burden of Disease Attributable to Ambient Air Pollution: An Analysis of Data from the Global Burden of Diseases Study 2015. *Lancet* **2017**, *389* (10082), 1907–1918. https://doi.org/10.1016/S0140-6736(17)30505-6.

(5) Guenther, A. B.; Jiang, X.; Heald, C. L.; Sakulyanontvittaya, T.; Duhl, T.; Emmons, L. K.; Wang, X. The Model of Emissions of Gases and Aerosols from Nature Version 2.1 (MEGAN2.1): An Extended and Updated Framework for Modeling Biogenic Emissions. *Geosci. Model Dev.* **2012**, *5* (6), 1471–1492. https://doi.org/10.5194/gmd-5-1471-2012.

(6) Hallquist, M.; Wenger, J. C.; Baltensperger, U.; Rudich, Y.; Simpson, D.; Claeys, M.; Dommen, J.; Donahue, N. M.; George, C.; Goldstein, A. H.; Hamilton, J. F.; Herrmann, H.; Hoffmann, T.; Iinuma, Y.; Jang, M.; Jenkin, M. E.; Jimenez, J. L.; Kiendler-Scharr, A.; Maenhaut, W.; McFiggans, G.; Mentel, Th. F.; Monod, A.; Prévôt, A. S. H.; Seinfeld, J. H.; Surratt, J. D.; Szmigielski, R.; Wildt, J. The Formation, Properties and Impact of Secondary Organic Aerosol: Current and Emerging Issues. *Atmos. Chem. Phys.* **2009**, *9* (14), 5155–5236. https://doi.org/10.5194/acp-9-5155-2009.

(7) Kanakidou, M.; Seinfeld, J. H.; Pandis, S. N.; Barnes, I.; Dentener, F. J.; Facchini, M. C.; Van Dingenen, R.; Ervens, B.; Nenes, A.; Nielsen, C. J.; Swietlicki, E.; Putaud, J. P.; Balkanski, Y.; Fuzzi, S.; Horth, J.; Moortgat, G. K.; Winterhalter, R.; Myhre, C. E. L.; Tsigaridis, K.; Vignati, E.; Stephanou, E. G.; Wilson, J. Organic Aerosol and Global Climate Modelling: A Review. *Atmos. Chem. Phys.* **2005**, *5* (4), 1053–1123. https://doi.org/10.5194/acp-5-1053-2005.

(8) Heald, C. L.; Henze, D. K.; Horowitz, L. W.; Feddema, J.; Lamarque, J.-F.; Guenther, A.; Hess, P. G.; Vitt, F.; Seinfeld, J. H.; Goldstein, A. H.; Fung, I. Predicted Change in Global Secondary Organic Aerosol Concentrations in Response to Future Climate, Emissions, and Land Use Change: FUTURE PREDICTED CHANGE IN GLOBAL SOA. *J. Geophys. Res.* **2008**, *113* (D5), n/a-n/a. https://doi.org/10.1029/2007JD009092.

(9) Zhang, H.; Yee, L. D.; Lee, B. H.; Curtis, M. P.; Worton, D. R.; Isaacman-VanWertz, G.; Offenberg, J. H.; Lewandowski, M.; Kleindienst, T. E.; Beaver, M. R.; Holder, A. L.; Lonneman, W. A.; Docherty, K. S.; Jaoui, M.; Pye, H. O. T.; Hu, W.; Day, D. A.; Campuzano-Jost, P.; Jimenez, J. L.; Guo, H.; Weber, R. J.; de Gouw, J.; Koss, A. R.; Edgerton, E. S.; Brune, W.; Mohr, C.; Lopez-Hilfiker, F. D.; Lutz, A.; Kreisberg, N. M.; Spielman, S. R.; Hering, S. V.; Wilson, K. R.; Thornton, J. A.; Goldstein, A. H. Monoterpenes Are the Largest Source of Summertime Organic Aerosol in the Southeastern United States. *Proc Natl Acad Sci USA* **2018**, *115* (9), 2038–2043. https://doi.org/10.1073/pnas.1717513115.

(10) Nozière, B.; Kalberer, M.; Claeys, M.; Allan, J.; D'Anna, B.; Decesari, S.; Finessi, E.; Glasius, M.; Grgić, I.; Hamilton, J. F.; Hoffmann, T.; Iinuma, Y.; Jaoui, M.; Kahnt, A.; Kampf, C. J.; Kourtchev, I.; Maenhaut, W.; Marsden, N.; Saarikoski, S.; Schnelle-Kreis, J.; Surratt, J. D.; Szidat, S.; Szmigielski, R.; Wisthaler, A. The Molecular Identification of Organic Compounds in the Atmosphere: State of the Art and Challenges. *Chem. Rev.* **2015**, *115* (10), 3919–3983. https://doi.org/10.1021/cr5003485.

(11) Laskin, J.; Laskin, A.; Nizkorodov, S. A. Mass Spectrometry Analysis in Atmospheric Chemistry. *Anal. Chem.* **2018**, *90* (1), 166–189. https://doi.org/10.1021/acs.analchem.7b04249.

(12) Reinhardt, A.; Emmenegger, C.; Gerrits, B.; Panse, C.; Dommen, J.; Baltensperger, U.; Zenobi, R.; Kalberer, M. Ultrahigh Mass Resolution and Accurate Mass Measurements as a Tool To Characterize Oligomers in Secondary Organic Aerosols. *Anal. Chem.* **2007**, *79* (11), 4074–4082. https://doi.org/10.1021/ac062425v.

(13) Müller, L.; Reinnig, M.-C.; Warnke, J.; Hoffmann, Th. Unambiguous Identification of Esters as Oligomers in Secondary Organic Aerosol Formed from Cyclohexene and Cyclohexene/α-Pinene Ozonolysis. *Atmos. Chem. Phys.* **2008**, *8* (5), 1423–1433. https://doi.org/10.5194/acp-8-1423-2008.

(14) Müller, L.; Reinnig, M.-C.; Hayen, H.; Hoffmann, T. Characterization of Oligomeric Compounds in Secondary Organic Aerosol Using Liquid Chromatography Coupled to Electrospray Ionization Fourier Transform Ion Cyclotron Resonance Mass Spectrometry. *Rapid Commun. Mass Spectrom.* **2009**, *23* (7), 971–979. https://doi.org/10.1002/rcm.3957.

(15) Camredon, M.; Hamilton, J. F.; Alam, M. S.; Wyche, K. P.; Carr, T.; White, I. R.; Monks, P. S.; Rickard, A. R.; Bloss, W. J. Distribution of Gaseous and Particulate Organic Composition during Dark α-Pinene Ozonolysis. *Atmos. Chem. Phys.* **2010**, *10* (6), 2893–2917. https://doi.org/10.5194/acp-10-2893-2010.

(16) Claeys, M.; Iinuma, Y.; Szmigielski, R.; Surratt, J. D.; Blockhuys, F.; Van Alsenoy, C.; Böge, O.; Sierau, B.; Gómez-González, Y.; Vermeylen, R.; Van der Veken, P.; Shahgholi, M.; Chan, A. W. H.; Herrmann, H.; Seinfeld, J. H.; Maenhaut, W. Terpenylic Acid and Related Compounds from the Oxidation of α-Pinene: Implications for New Particle Formation and Growth above Forests. *Environ. Sci. Technol.* **2009**, *43* (18), 6976–6982. https://doi.org/10.1021/es9007596.

(17) Yasmeen, F.; Vermeylen, R.; Szmigielski, R.; Iinuma, Y.; Böge, O.; Herrmann, H.; Maenhaut, W.; Claeys, M. Terpenylic Acid and Related Compounds: Precursors for Dimers in Secondary Organic Aerosol from the Ozonolysis of α- and β-Pinene. *Atmos. Chem. Phys.* **2010**, *10* (19), 9383–9392. https://doi.org/10.5194/acp-10-9383-2010.

(18) Yasmeen, F.; Szmigielski, R.; Vermeylen, R.; Gómez-González, Y.; Surratt, J. D.; Chan, A. W. H.; Seinfeld, J. H.; Maenhaut, W.; Claeys, M. Mass Spectrometric Characterization of Isomeric Terpenoic Acids from the Oxidation of α-Pinene, β-Pinene, d-Limonene, and Δ3-Carene in Fine Forest Aerosol. *J. Mass Spectrom.* **2011**, *46* (4), 425–442. https://doi.org/10.1002/jms.1911.

(19) Yasmeen, F.; Vermeylen, R.; Maurin, N.; Perraudin, E.; Doussin, J.-F.; Claeys, M. Characterisation of Tracers for Aging of α-Pinene Secondary Organic Aerosol Using Liquid Chromatography/Negative Ion Electrospray Ionisation Mass Spectrometry. *Environ. Chem.* **2012**, *9* (3), 236. https://doi.org/10.1071/EN11148.

(20) Gao, Y.; Hall, W. A.; Johnston, M. V. Molecular Composition of Monoterpene Secondary Organic Aerosol at Low Mass Loading. *Environ. Sci. Technol.* **2010**, *44* (20), 7897–7902. https://doi.org/10.1021/es101861k.

(21) Hall, W. A.; Johnston, M. V. Oligomer Content of α-Pinene Secondary Organic Aerosol. *Aerosol Science and Technology* **2011**, *45* (1), 37–45. https://doi.org/10.1080/02786826.2010.517580.

(22) Putman, A. L.; Offenberg, J. H.; Fisseha, R.; Kundu, S.; Rahn, T. A.; Mazzoleni, L. R. Ultrahigh-Resolution FT-ICR Mass Spectrometry Characterization of α-Pinene Ozonolysis SOA. *Atmospheric Environment* **2012**, *46*, 164–172. https://doi.org/10.1016/j.atmosenv.2011.10.003.

(23) Witkowski, B.; Gierczak, T. Early Stage Composition of SOA Produced by α-Pinene/Ozone Reaction: α-Acyloxyhydroperoxy Aldehydes and Acidic Dimers. *Atmospheric Environment* **2014**, *95*, 59–70. https://doi.org/10.1016/j.atmosenv.2014.06.018.

(24) Kourtchev, I.; Fuller, S. J.; Giorio, C.; Healy, R. M.; Wilson, E.; O'Connor, I.; Wenger, J. C.; McLeod, M.; Aalto, J.; Ruuskanen, T. M.; Maenhaut, W.; Jones, R.; Venables, D. S.; Sodeau, J. R.; Kulmala, M.; Kalberer, M. Molecular Composition of Biogenic Secondary Organic Aerosols Using Ultrahigh-Resolution Mass Spectrometry: Comparing Laboratory and Field Studies. *Atmos. Chem. Phys.* **2014**, *14* (4), 2155–2167. https://doi.org/10.5194/acp-14-2155-2014.

(25) Kourtchev, I.; Doussin, J.-F.; Giorio, C.; Mahon, B.; Wilson, E. M.; Maurin, N.; Pangui, E.; Venables, D. S.; Wenger, J. C.; Kalberer, M. Molecular Composition of Fresh and Aged Secondary Organic Aerosol from a Mixture of Biogenic Volatile Compounds: A High-Resolution Mass Spectrometry Study. *Atmos. Chem. Phys.* **2015**, *15* (10), 5683–5695. https://doi.org/10.5194/acp-15-5683-2015.

(26) Kourtchev, I.; Giorio, C.; Manninen, A.; Wilson, E.; Mahon, B.; Aalto, J.; Kajos, M.; Venables, D.; Ruuskanen, T.; Levula, J.; Loponen, M.; Connors, S.; Harris, N.; Zhao, D.; Kiendler-Scharr, A.; Mentel, T.; Rudich, Y.; Hallquist, M.; Doussin, J.-F.; Maenhaut, W.; Bäck, J.; Petäjä, T.; Wenger, J.; Kulmala, M.; Kalberer, M. Enhanced Volatile Organic Compounds Emissions and Organic Aerosol Mass Increase the Oligomer Content of Atmospheric Aerosols. *Sci Rep* **2016**, *6* (1), 35038. https://doi.org/10.1038/srep35038.

(27) Kristensen, K.; Enggrob, K. L.; King, S. M.; Worton, D. R.; Platt, S. M.; Mortensen, R.; Rosenoern, T.; Surratt, J. D.; Bilde, M.; Goldstein, A. H.; Glasius, M. Formation and

Occurrence of Dimer Esters of Pinene Oxidation Products in Atmospheric Aerosols. *Atmos. Chem. Phys.* **2013**, *13* (7), 3763–3776. https://doi.org/10.5194/acp-13-3763-2013.

(28) Kristensen, K.; Cui, T.; Zhang, H.; Gold, A.; Glasius, M.; Surratt, J. D. Dimers in α-Pinene Secondary Organic Aerosol: Effect of Hydroxyl Radical, Ozone, Relative Humidity and Aerosol Acidity. *Atmos. Chem. Phys.* **2014**, *14* (8), 4201–4218. https://doi.org/10.5194/acp-14-4201-2014.

(29) Kristensen, K.; Watne, Å. K.; Hammes, J.; Lutz, A.; Petäjä, T.; Hallquist, M.; Bilde, M.; Glasius, M. High-Molecular Weight Dimer Esters Are Major Products in Aerosols from α-Pinene Ozonolysis and the Boreal Forest. *Environ. Sci. Technol. Lett.* **2016**, *3* (8), 280–285. https://doi.org/10.1021/acs.estlett.6b00152.

(30) Kristensen, K.; Jensen, L. N.; Glasius, M.; Bilde, M. The Effect of Sub-Zero Temperature on the Formation and Composition of Secondary Organic Aerosol from Ozonolysis of Alpha-Pinene. *Environ. Sci.: Processes Impacts* **2017**, *19* (10), 1220–1234. https://doi.org/10.1039/C7EM00231A.

(31) Zhang, X.; McVay, R. C.; Huang, D. D.; Dalleska, N. F.; Aumont, B.; Flagan, R. C.; Seinfeld, J. H. Formation and Evolution of Molecular Products in α-Pinene Secondary Organic Aerosol. *Proc Natl Acad Sci USA* **2015**, *112* (46), 14168–14173. https://doi.org/10.1073/pnas.1517742112.

(32) Sato, K.; Jia, T.; Tanabe, K.; Morino, Y.; Kajii, Y.; Imamura, T. Terpenylic Acid and Nine-Carbon Multifunctional Compounds Formed during the Aging of β-Pinene Ozonolysis Secondary Organic Aerosol. *Atmospheric Environment* **2016**, *130*, 127–135. https://doi.org/10.1016/j.atmosenv.2015.08.047.

(33) Mutzel, A.; Rodigast, M.; Iinuma, Y.; Böge, O.; Herrmann, H. Monoterpene SOA – Contribution of First-Generation Oxidation Products to Formation and Chemical Composition. *Atmospheric Environment* **2016**, *130*, 136–144. https://doi.org/10.1016/j.atmosenv.2015.10.080.

(34) Kenseth, C. M.; Huang, Y.; Zhao, R.; Dalleska, N. F.; Hethcox, J. C.; Stoltz, B. M.; Seinfeld, J. H. Synergistic O3 + OH Oxidation Pathway to Extremely Low-Volatility Dimers Revealed in β-Pinene Secondary Organic Aerosol. *Proc Natl Acad Sci USA* **2018**, *115* (33), 8301–8306. https://doi.org/10.1073/pnas.1804671115.

(35) Zhao, R.; Kenseth, C. M.; Huang, Y.; Dalleska, N. F.; Seinfeld, J. H. Iodometry-Assisted Liquid Chromatography Electrospray Ionization Mass Spectrometry for Analysis of Organic Peroxides: An Application to Atmospheric Secondary Organic Aerosol. *Environ. Sci. Technol.* **2018**, *52* (4), 2108–2117. https://doi.org/10.1021/acs.est.7b04863.

(36) Kahnt, A.; Vermeylen, R.; Iinuma, Y.; Safi Shalamzari, M.; Maenhaut, W.; Claeys, M. High-Molecular-Weight Esters in α-Pinene Ozonolysis Secondary Organic Aerosol: Structural Characterization and Mechanistic Proposal for Their Formation from Highly Oxygenated Molecules. *Atmos. Chem. Phys.* **2018**, *18* (11), 8453–8467. https://doi.org/10.5194/acp-18-8453-2018.

(37) Sato, K.; Fujitani, Y.; Inomata, S.; Morino, Y.; Tanabe, K.; Ramasamy, S.; Hikida, T.; Shimono, A.; Takami, A.; Fushimi, A.; Kondo, Y.; Imamura, T.; Tanimoto, H.; Sugata, S. Studying Volatility from Composition, Dilution, and Heating Measurements of Secondary Organic Aerosols Formed during <I>α</I>-Pinene Ozonolysis. *Atmos. Chem. Phys.* **2018**, *18* (8), 5455–5466. https://doi.org/10.5194/acp-18-5455-2018.

(38) Wozniak, A. S.; Bauer, J. E.; Sleighter, R. L.; Dickhut, R. M.; Hatcher, P. G. Technical Note: Molecular Characterization of Aerosol-Derived Water Soluble Organic Carbon Using

Ultrahigh Resolution Electrospray Ionization Fourier Transform Ion Cyclotron Resonance Mass Spectrometry. *Atmos. Chem. Phys.* **2008**, *8* (17), 5099–5111. https://doi.org/10.5194/acp-8-5099-2008.

(39) Konermann, L.; Ahadi, E.; Rodriguez, A. D.; Vahidi, S. Unraveling the Mechanism of Electrospray Ionization. *Anal. Chem.* **2013**, *85* (1), 2–9. https://doi.org/10.1021/ac302789c.

(40) Oss, M.; Kruve, A.; Herodes, K.; Leito, I. Electrospray Ionization Efficiency Scale of Organic Compounds. *Anal. Chem.* **2010**, *82* (7), 2865–2872. https://doi.org/10.1021/ac902856t.

(41) Kruve, A.; Kaupmees, K.; Liigand, J.; Leito, I. Negative Electrospray Ionization via Deprotonation: Predicting the Ionization Efficiency. *Anal. Chem.* **2014**, *86* (10), 4822–4830. https://doi.org/10.1021/ac404066v.

(42) Kruve, A.; Kaupmees, K. Predicting ESI/MS Signal Change for Anions in Different Solvents. *Anal. Chem.* **2017**, *89* (9), 5079–5086. https://doi.org/10.1021/acs.analchem.7b00595.

(43) Moglioni, A. G.; García-Expósito, E.; Aguado, G. P.; Parella, T.; Branchadell, V.; Moltrasio, G. Y.; Ortuño, R. M. Divergent Routes to Chiral Cyclobutane Synthons from (−)-α-Pinene and Their Use in the Stereoselective Synthesis of Dehydro Amino Acids. *J. Org. Chem.* **2000**, *65* (13), 3934–3940. https://doi.org/10.1021/jo991773c.

(44) Hergueta, A. R.; López, C.; Fernández, F.; Caamaño, O.; Blanco, J. M. Synthesis of Two Enantiomerically Pure Precursors of Cyclobutane Carbocyclic Nucleosides. *Tetrahedron: Asymmetry* **2003**, *14* (23), 3773–3778. https://doi.org/10.1016/j.tetasy.2003.09.033.

(45) Schwantes, R. H.; McVay, R. C.; Zhang, X.; Coggon, M. M.; Lignell, H.; Flagan, R. C.; Wennberg, P. O.; Seinfeld, J. H. Science of the Environmental Chamber. In *Advances in Atmospheric Chemistry*; Barker, J. R., Steiner, A. L., Wallington, T. J., Eds.; World Scientific: Singapore, 2017; pp 1–93. https://doi.org/10.1142/9789813147355_0001.

(46) Aschmann, S. M.; Arey, J.; Atkinson, R. OH Radical Formation from the Gas-Phase Reactions of O3 with a Series of Terpenes. *Atmospheric Environment* **2002**, *36* (27), 4347–4355. https://doi.org/10.1016/S1352-2310(02)00355-2.

(47) Presto, A. A.; Donahue, N. M. Ozonolysis Fragment Quenching by Nitrate Formation: The Pressure Dependence of Prompt OH Radical Formation. *J. Phys. Chem. A* **2004**, *108* (42), 9096–9104. https://doi.org/10.1021/jp047162s.

(48) Ma, Y.; Marston, G. Multifunctional Acid Formation from the Gas-Phase Ozonolysis of β-Pinene. *Phys. Chem. Chem. Phys.* **2008**, *10* (40), 6115. https://doi.org/10.1039/b807863g.

(49) Nguyen, T. L.; Peeters, J.; Vereecken, L. Theoretical Study of the Gas-Phase Ozonolysis of β-Pinene (C10H16). *Phys. Chem. Chem. Phys.* **2009**, *11* (27), 5643. https://doi.org/10.1039/b822984h.

(50) Schwantes, R. H.; Charan, S. M.; Bates, K. H.; Huang, Y.; Nguyen, T. B.; Mai, H.; Kong, W.; Flagan, R. C.; Seinfeld, J. H. Low-Volatility Compounds Contribute Significantly to Isoprene Secondary Organic Aerosol (SOA) under High-NO_x Conditions. *Atmos. Chem. Phys.* **2019**, *19* (11), 7255–7278. https://doi.org/10.5194/acp-19-7255-2019.

(51) Bahreini, R.; Keywood, M. D.; Ng, N. L.; Varutbangkul, V.; Gao, S.; Flagan, R. C.; Seinfeld, J. H.; Worsnop, D. R.; Jimenez, J. L. Measurements of Secondary Organic Aerosol from Oxidation of Cycloalkenes, Terpenes, and *m* -Xylene Using an Aerodyne Aerosol Mass Spectrometer. *Environ. Sci. Technol.* **2005**, *39* (15), 5674–5688. https://doi.org/10.1021/es048061a.

(52) Malloy, Q. G. J.; Nakao, S.; Qi, L.; Austin, R.; Stothers, C.; Hagino, H.; Cocker, D. R. Real-Time Aerosol Density Determination Utilizing a Modified Scanning Mobility Particle

Sizer—Aerosol Particle Mass Analyzer System. *Aerosol Science and Technology* **2009**, *43* (7), 673–678. https://doi.org/10.1080/02786820902832960.

(53) Shilling, J. E.; Chen, Q.; King, S. M.; Rosenoern, T.; Kroll, J. H.; Worsnop, D. R.; DeCarlo, P. F.; Aiken, A. C.; Sueper, D.; Jimenez, J. L.; Martin, S. T. Loading-Dependent Elemental Composition of α-Pinene SOA Particles. *Atmos. Chem. Phys.* **2009**, *9* (3), 771–782. https://doi.org/10.5194/acp-9-771-2009.

(54) Saathoff, H.; Naumann, K.-H.; Möhler, O.; Jonsson, Å. M.; Hallquist, M.; Kiendler-Scharr, A.; Mentel, Th. F.; Tillmann, R.; Schurath, U. Temperature Dependence of Yields of Secondary Organic Aerosols from the Ozonolysis of α -Pinene and Limonene. *Atmos. Chem. Phys.* **2009**, *9* (5), 1551–1577. https://doi.org/10.5194/acp-9-1551-2009.

(55) DeCarlo, P. F.; Kimmel, J. R.; Trimborn, A.; Northway, M. J.; Jayne, J. T.; Aiken, A. C.; Gonin, M.; Fuhrer, K.; Horvath, T.; Docherty, K. S.; Worsnop, D. R.; Jimenez, J. L. Field-Deployable, High-Resolution, Time-of-Flight Aerosol Mass Spectrometer. *Anal. Chem.* **2006**, *78* (24), 8281–8289. https://doi.org/10.1021/ac061249n.

(56) Allan, J. D.; Delia, A. E.; Coe, H.; Bower, K. N.; Alfarra, M. R.; Jimenez, J. L.; Middlebrook, A. M.; Drewnick, F.; Onasch, T. B.; Canagaratna, M. R.; Jayne, J. T.; Worsnop, D. R. A Generalised Method for the Extraction of Chemically Resolved Mass Spectra from Aerodyne Aerosol Mass Spectrometer Data. *Journal of Aerosol Science* **2004**, *35* (7), 909–922. https://doi.org/10.1016/j.jaerosci.2004.02.007.

(57) Aiken, A. C.; DeCarlo, P. F.; Kroll, J. H.; Worsnop, D. R.; Huffman, J. A.; Docherty, K. S.; Ulbrich, I. M.; Mohr, C.; Kimmel, J. R.; Sueper, D.; Sun, Y.; Zhang, Q.; Trimborn, A.; Northway, M.; Ziemann, P. J.; Canagaratna, M. R.; Onasch, T. B.; Alfarra, M. R.; Prevot, A. S. H.; Dommen, J.; Duplissy, J.; Metzger, A.; Baltensperger, U.; Jimenez, J. L. O/C and OM/OC Ratios of Primary, Secondary, and Ambient Organic Aerosols with High-Resolution Time-of-Flight Aerosol Mass Spectrometry. *Environ. Sci. Technol.* **2008**, *42* (12), 4478–4485. https://doi.org/10.1021/es703009q.

(58) Middlebrook, A. M.; Bahreini, R.; Jimenez, J. L.; Canagaratna, M. R. Evaluation of Composition-Dependent Collection Efficiencies for the Aerodyne Aerosol Mass Spectrometer Using Field Data. *Aerosol Science and Technology* **2012**, *46* (3), 258–271. https://doi.org/10.1080/02786826.2011.620041.

(59) Canagaratna, M. R.; Jimenez, J. L.; Kroll, J. H.; Chen, Q.; Kessler, S. H.; Massoli, P.; Hildebrandt Ruiz, L.; Fortner, E.; Williams, L. R.; Wilson, K. R.; Surratt, J. D.; Donahue, N. M.; Jayne, J. T.; Worsnop, D. R. Elemental Ratio Measurements of Organic Compounds Using Aerosol Mass Spectrometry: Characterization, Improved Calibration, and Implications. *Atmos. Chem. Phys.* **2015**, *15* (1), 253–272. https://doi.org/10.5194/acp-15-253-2015.

(60) Chhabra, P. S.; Flagan, R. C.; Seinfeld, J. H. Elemental Analysis of Chamber Organic Aerosol Using an Aerodyne High-Resolution Aerosol Mass Spectrometer. *Atmos. Chem. Phys.* **2010**, *10* (9), 4111–4131. https://doi.org/10.5194/acp-10-4111-2010.

(61) Chen, Q.; Liu, Y.; Donahue, N. M.; Shilling, J. E.; Martin, S. T. Particle-Phase Chemistry of Secondary Organic Material: Modeled Compared to Measured O:C and H:C Elemental Ratios Provide Constraints. *Environ. Sci. Technol.* **2011**, *45* (11), 4763–4770. https://doi.org/10.1021/es104398s.

(62) Donahue, N. M.; Henry, K. M.; Mentel, T. F.; Kiendler-Scharr, A.; Spindler, C.; Bohn, B.; Brauers, T.; Dorn, H. P.; Fuchs, H.; Tillmann, R.; Wahner, A.; Saathoff, H.; Naumann, K.-H.; Mohler, O.; Leisner, T.; Muller, L.; Reinnig, M.-C.; Hoffmann, T.; Salo, K.; Hallquist,

M.; Frosch, M.; Bilde, M.; Tritscher, T.; Barmet, P.; Praplan, A. P.; DeCarlo, P. F.; Dommen, J.; Prevot, A. S. H.; Baltensperger, U. Aging of Biogenic Secondary Organic Aerosol via Gas-Phase OH Radical Reactions. *Proceedings of the National Academy of Sciences* **2012**, *109* (34), 13503–13508. https://doi.org/10.1073/pnas.1115186109.

(63) Nakao, S.; Tang, P.; Tang, X.; Clark, C. H.; Qi, L.; Seo, E.; Asa-Awuku, A.; Cocker, D. Density and Elemental Ratios of Secondary Organic Aerosol: Application of a Density Prediction Method. *Atmospheric Environment* **2013**, *68*, 273–277. https://doi.org/10.1016/j.atmosenv.2012.11.006.

(64) Sorooshian, A.; Brechtel, F. J.; Ma, Y.; Weber, R. J.; Corless, A.; Flagan, R. C.; Seinfeld, J. H. Modeling and Characterization of a Particle-into-Liquid Sampler (PILS). *Aerosol Science and Technology* **2006**, *40* (6), 396–409. https://doi.org/10.1080/02786820600632282.

(65) Zhang, X.; Dalleska, N. F.; Huang, D. D.; Bates, K. H.; Sorooshian, A.; Flagan, R. C.; Seinfeld, J. H. Time-Resolved Molecular Characterization of Organic Aerosols by PILS + UPLC/ESI-Q-TOFMS. *Atmospheric Environment* **2016**, *130*, 180–189. https://doi.org/10.1016/j.atmosenv.2015.08.049.

(66) Ryerson, T. B.; Andrews, A. E.; Angevine, W. M.; Bates, T. S.; Brock, C. A.; Cairns, B.; Cohen, R. C.; Cooper, O. R.; de Gouw, J. A.; Fehsenfeld, F. C.; Ferrare, R. A.; Fischer, M. L.; Flagan, R. C.; Goldstein, A. H.; Hair, J. W.; Hardesty, R. M.; Hostetler, C. A.; Jimenez, J. L.; Langford, A. O.; McCauley, E.; McKeen, S. A.; Molina, L. T.; Nenes, A.; Oltmans, S. J.; Parrish, D. D.; Pederson, J. R.; Pierce, R. B.; Prather, K.; Quinn, P. K.; Seinfeld, J. H.; Senff, C. J.; Sorooshian, A.; Stutz, J.; Surratt, J. D.; Trainer, M.; Volkamer, R.; Williams, E. J.; Wofsy, S. C. The 2010 California Research at the Nexus of Air Quality and Climate Change (CalNex) Field Study: CalNex 2010 FIELD PROJECT OVERVIEW. *J. Geophys. Res. Atmos.* **2013**, *118* (11), 5830–5866. https://doi.org/10.1002/jgrd.50331.

(67) Lopez-Hilfiker, F. D.; Mohr, C.; Ehn, M.; Rubach, F.; Kleist, E.; Wildt, J.; Mentel, Th. F.; Carrasquillo, A. J.; Daumit, K. E.; Hunter, J. F.; Kroll, J. H.; Worsnop, D. R.; Thornton, J. A. Phase Partitioning and Volatility of Secondary Organic Aerosol Components Formed from α-Pinene Ozonolysis and OH Oxidation: The Importance of Accretion Products and Other Low Volatility Compounds. *Atmos. Chem. Phys.* **2015**, *15* (14), 7765–7776. https://doi.org/10.5194/acp-15-7765-2015.

(68) Yatavelli, R. L. N.; Mohr, C.; Stark, H.; Day, D. A.; Thompson, S. L.; Lopez-Hilfiker, F. D.; Campuzano-Jost, P.; Palm, B. B.; Vogel, A. L.; Hoffmann, T.; Heikkinen, L.; Äijälä, M.; Ng, N. L.; Kimmel, J. R.; Canagaratna, M. R.; Ehn, M.; Junninen, H.; Cubison, M. J.; Petäjä, T.; Kulmala, M.; Jayne, J. T.; Worsnop, D. R.; Jimenez, J. L. Estimating the Contribution of Organic Acids to Northern Hemispheric Continental Organic Aerosol: ORGANIC ACID CONTRIBUTION TO OA. *Geophys. Res. Lett.* **2015**, *42* (14), 6084–6090. https://doi.org/10.1002/2015GL064650.

(69) Ma, Y.; Russell, A. T.; Marston, G. Mechanisms for the Formation of Secondary Organic Aerosol Components from the Gas-Phase Ozonolysis of α-Pinene. *Phys. Chem. Chem. Phys.* **2008**, *10* (29), 4294. https://doi.org/10.1039/b803283a.

(70) Atkinson, R.; Arey, J. Atmospheric Degradation of Volatile Organic Compounds. *Chem. Rev.* **2003**, *103* (12), 4605–4638. https://doi.org/10.1021/cr0206420.

(71) Ehn, M.; Thornton, J. A.; Kleist, E.; Sipilä, M.; Junninen, H.; Pullinen, I.; Springer, M.; Rubach, F.; Tillmann, R.; Lee, B.; Lopez-Hilfiker, F.; Andres, S.; Acir, I.-H.; Rissanen, M.; Jokinen, T.; Schobesberger, S.; Kangasluoma, J.; Kontkanen, J.; Nieminen, T.; Kurtén, T.;

Nielsen, L. B.; Jørgensen, S.; Kjaergaard, H. G.; Canagaratna, M.; Maso, M. D.; Berndt, T.; Petäjä, T.; Wahner, A.; Kerminen, V.-M.; Kulmala, M.; Worsnop, D. R.; Wildt, J.; Mentel, T. F. A Large Source of Low-Volatility Secondary Organic Aerosol. *Nature* **2014**, *506* (7489), 476–479. https://doi.org/10.1038/nature13032.

(72) Donahue, N. M.; Epstein, S. A.; Pandis, S. N.; Robinson, A. L. A Two-Dimensional Volatility Basis Set: 1. Organic-Aerosol Mixing Thermodynamics. *Atmos. Chem. Phys.* **2011**, *11* (7), 3303–3318. https://doi.org/10.5194/acp-11-3303-2011.

(73) Bianchi, F.; Kurtén, T.; Riva, M.; Mohr, C.; Rissanen, M. P.; Roldin, P.; Berndt, T.; Crounse, J. D.; Wennberg, P. O.; Mentel, T. F.; Wildt, J.; Junninen, H.; Jokinen, T.; Kulmala, M.; Worsnop, D. R.; Thornton, J. A.; Donahue, N.; Kjaergaard, H. G.; Ehn, M. Highly Oxygenated Organic Molecules (HOM) from Gas-Phase Autoxidation Involving Peroxy Radicals: A Key Contributor to Atmospheric Aerosol. *Chem. Rev.* **2019**, *119* (6), 3472–3509. https://doi.org/10.1021/acs.chemrev.8b00395.

(74) Jokinen, T.; Berndt, T.; Makkonen, R.; Kerminen, V.-M.; Junninen, H.; Paasonen, P.; Stratmann, F.; Herrmann, H.; Guenther, A. B.; Worsnop, D. R.; Kulmala, M.; Ehn, M.; Sipilä, M. Production of Extremely Low Volatile Organic Compounds from Biogenic Emissions: Measured Yields and Atmospheric Implications. *Proc Natl Acad Sci USA* **2015**, *112* (23), 7123–7128. https://doi.org/10.1073/pnas.1423977112.

(75) Zhang, X.; Lambe, A. T.; Upshur, M. A.; Brooks, W. A.; Gray Bé, A.; Thomson, R. J.; Geiger, F. M.; Surratt, J. D.; Zhang, Z.; Gold, A.; Graf, S.; Cubison, M. J.; Groessl, M.; Jayne, J. T.; Worsnop, D. R.; Canagaratna, M. R. Highly Oxygenated Multifunctional Compounds in α-Pinene Secondary Organic Aerosol. *Environ. Sci. Technol.* **2017**, *51* (11), 5932–5940. https://doi.org/10.1021/acs.est.6b06588.

(76) Zhao, Y.; Thornton, J. A.; Pye, H. O. T. Quantitative Constraints on Autoxidation and Dimer Formation from Direct Probing of Monoterpene-Derived Peroxy Radical Chemistry. *Proc Natl Acad Sci USA* **2018**, *115* (48), 12142–12147. https://doi.org/10.1073/pnas.1812147115.

(77) Li, H.; Chen, Z.; Huang, L.; Huang, D. Organic Peroxides' Gas-Particle Partitioning and Rapid Heterogeneous Decomposition on Secondary Organic Aerosol. *Atmos. Chem. Phys.* **2016**, *16* (3), 1837–1848. https://doi.org/10.5194/acp-16-1837-2016.

(78) Krapf, M.; El Haddad, I.; Bruns, E. A.; Molteni, U.; Daellenbach, K. R.; Prévôt, A. S. H.; Baltensperger, U.; Dommen, J. Labile Peroxides in Secondary Organic Aerosol. *Chem* **2016**, *1* (4), 603–616. https://doi.org/10.1016/j.chempr.2016.09.007.

(79) Riva, M.; Budisulistiorini, S. H.; Zhang, Z.; Gold, A.; Thornton, J. A.; Turpin, B. J.; Surratt, J. D. Multiphase Reactivity of Gaseous Hydroperoxide Oligomers Produced from Isoprene Ozonolysis in the Presence of Acidified Aerosols. *Atmospheric Environment* **2017**, *152*, 314–322. https://doi.org/10.1016/j.atmosenv.2016.12.040.

(80) Zhao, R.; Kenseth, C. M.; Huang, Y.; Dalleska, N. F.; Kuang, X. M.; Chen, J.; Paulson, S. E.; Seinfeld, J. H. Rapid Aqueous-Phase Hydrolysis of Ester Hydroperoxides Arising from Criegee Intermediates and Organic Acids. *J. Phys. Chem. A* **2018**, *122* (23), 5190–5201. https://doi.org/10.1021/acs.jpca.8b02195.

(81) Docherty, K. S.; Wu, W.; Lim, Y. B.; Ziemann, P. J. Contributions of Organic Peroxides to Secondary Aerosol Formed from Reactions of Monoterpenes with O_3. *Environ. Sci. Technol.* **2005**, *39* (11), 4049–4059. https://doi.org/10.1021/es050228s.

(82) Claflin, M. S.; Krechmer, J. E.; Hu, W.; Jimenez, J. L.; Ziemann, P. J. Functional Group Composition of Secondary Organic Aerosol Formed from Ozonolysis of α-Pinene Under

High VOC and Autoxidation Conditions. *ACS Earth Space Chem.* **2018**, *2* (11), 1196–1210. https://doi.org/10.1021/acsearthspacechem.8b00117.

(83) Li, X.; Chee, S.; Hao, J.; Abbatt, J. P. D.; Jiang, J.; Smith, J. N. Relative Humidity Effect on the Formation of Highly Oxidized Molecules and New Particles during Monoterpene Oxidation. *Atmos. Chem. Phys.* **2019**, *19* (3), 1555–1570. https://doi.org/10.5194/acp-19-1555-2019.

(84) Berndt, T.; Mentler, B.; Scholz, W.; Fischer, L.; Herrmann, H.; Kulmala, M.; Hansel, A. Accretion Product Formation from Ozonolysis and OH Radical Reaction of α-Pinene: Mechanistic Insight and the Influence of Isoprene and Ethylene. *Environ. Sci. Technol.* **2018**, *52* (19), 11069–11077. https://doi.org/10.1021/acs.est.8b02210.

TABLES AND FIGURES

Table 1. Initial conditions and SOA properties for α-pinene and β-pinene ozonolysis experiments in the CTEC.[a,b]

VOC	Exp.	$[VOC]_0$ (ppb)	$[O_3]_0$ (ppb)	$[(NH_4)_2SO_4]_0$ (μm^3 cm^{-3})	[SOA] (μg m^{-3})[c]	Bulk O:C[c]	Bulk $\overline{OS}_C$[c,d]	SOA Mass Fraction (%)[c,e]		
								Monomer	Dimer	Total
α-Pinene	1–4	104 ± 5	150	86–223	232 ± 26	0.41 ± 0.01	−0.87 ± 0.02	20.5 ± 2.5	1.3 ± 0.1	21.8 ± 2.6
β-Pinene	5–9	95 ± 2	150	137–283	78 ± 14	0.36 ± 0.01	−0.92 ± 0.02	15.6 ± 2.7	3.3 ± 0.6	18.9 ± 3.2

[a]~5-h duration; T_0 = 295 ± 2 K; P = 1 atm; RH < 5%; $[NO_x]_0$ < 0.5 ppb; no OH scavenger.
[b]Data are reported as averages (1σ) of replicate experiments for α-pinene (n = 4) and β-pinene (n = 5).
[c]Calculated for suspended SOA after ~5 h of ozonolysis (see Figure 1).
[d]Average carbon oxidation state ($\overline{OS}_C$ = 2 O:C − H:C).
[e]Method uncertainty is estimated to be ±23% (relative). See Experimental for details.

Table 2. Mass fractions of molecular products in SOA from α-pinene ozonolysis quantified via LC/(−)ESI-MS.[a]

Reference	$[\alpha\text{-P}]_0$ (ppb)	$[O_3]_0$ (ppb)	$[(NH_4)_2SO_4]_0$ (μm^3 cm^{-3})	[SOA] (μg m^{-3})	Bulk O:C	Bulk $\overline{OS}_C$	SOA Mass Fraction (%)[c,d]			
							cis-Pinic Acid	Monomer	Dimer	Total
Zhang et al. (2015)[31]	154	200	73	120	0.45	−0.72	21.0 [5.3]	39.2 [26.0] (9)	6.5 [2.6] (13)	45.7 [28.6]
Kristensen et al. (2017)[30]	50	200	–	60	0.40	−0.85	4.5	20.5 (16)	8.6 [1.1] (30)	29.1 [21.6]
This Work[b]	104 ± 5	150	86–223	232 ± 26	0.41 ± 0.01	−0.87 ± 0.02	3.9 ± 0.6	20.5 ± 2.5 (36)	1.3 ± 0.1 (46)	21.8 ± 2.6

[a]Experiments in each study were carried out in batch-mode Teflon environmental chambers at 293–298 K and ~1 atm, under dry (<5% RH), low-NO_x (<1 ppb) conditions, and in the absence of an OH scavenger.
[b]See Table 1 for details.
[c]Bracketed values represent adjusted mass fraction estimates based on (−)ESI efficiencies derived in this work. Details are provided in SI, Section S1.
[d]Numbers of identified monomers and dimers are given in parentheses.

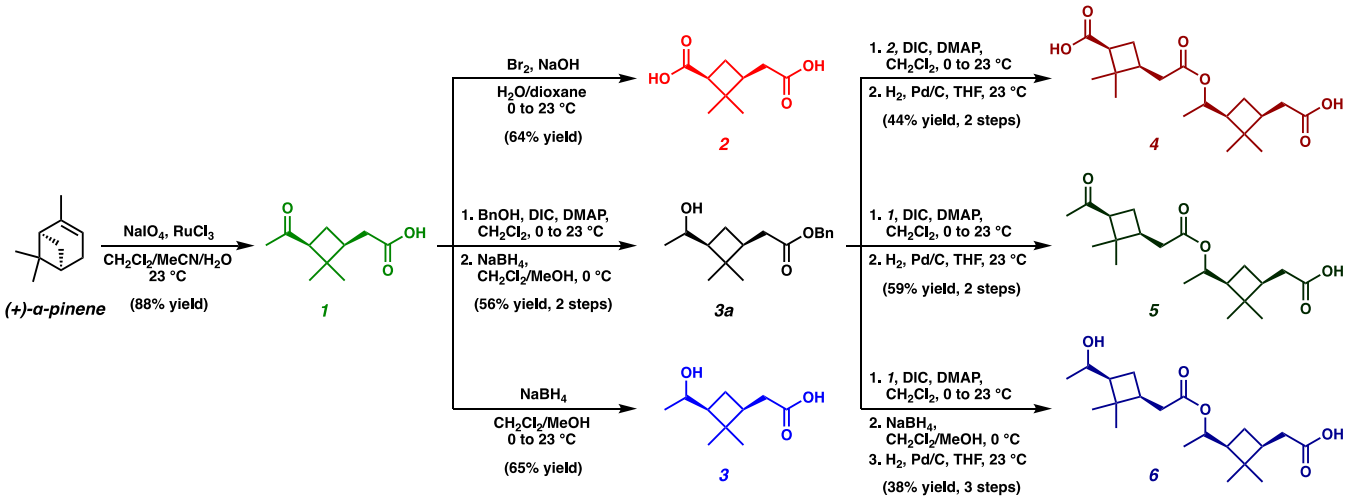

Scheme 1. Synthesis of carboxylic acids **1–3** and dimer esters **4–6** from commercially available (+)-α-pinene. In cases where epimers were generated via reduction of ketones with $NaBH_4$ (i.e., compounds **3**, **3a**, and **6**), only the major epimer was isolated but the relative stereochemistry remains unassigned.

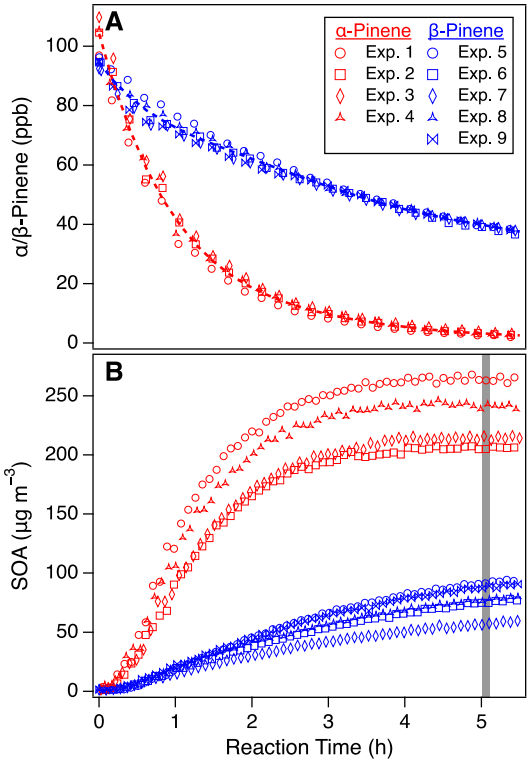

Figure 1. (A) GC/FID-derived decay curves and (B) SMPS-derived suspended SOA growth profiles for α-pinene and β-pinene ozonolysis experiments in the CTEC. Experimental conditions are reported in Table S1. Gray bar denotes 5-min interval for which SOA mass fractions and properties were calculated in each experiment.

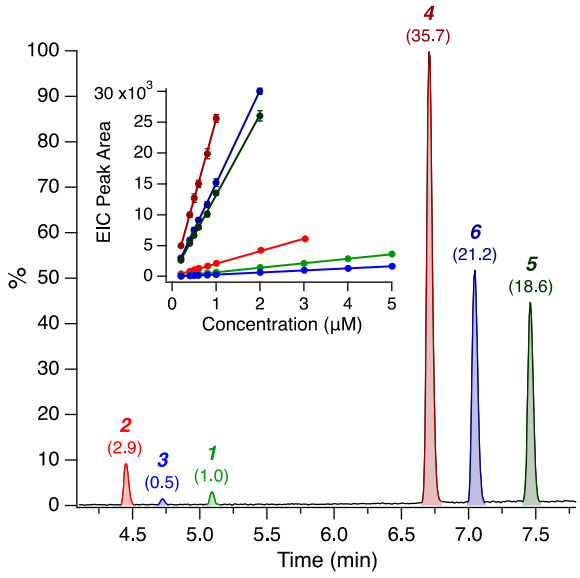

Figure 2. UPLC/(–)ESI-Q-TOF-MS BPI chromatogram of an equimolar (1.00 μM) aqueous solution of carboxylic acids **1**–**3** and dimer esters **4**–**6**. (–)ESI efficiencies, normalized to that of *cis*-pinonic acid (**1**), are given in parentheses. (Inset) Weighted (1/X), linear (R^2 > 0.998) calibration curves, generated from triplicate measurements (1σ) of equimolar aqueous solutions of carboxylic acids **1**–**3** and dimer esters **4**–**6** spanning a concentration range from 0.200 to 5.00 μM.

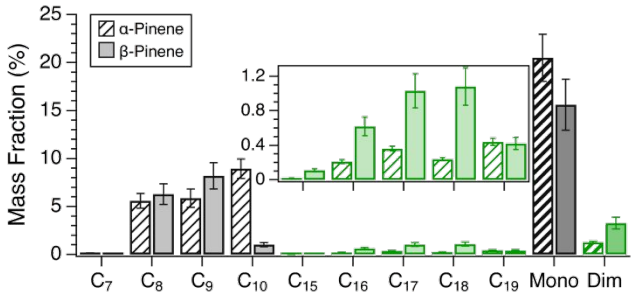

Figure 3. Mass fractions of molecular products identified in α-pinene and β-pinene SOA as a function of carbon number (n_C), calculated for suspended SOA after ~5 h of ozonolysis in the CTEC (see Figure 1) and reported as averages (1σ) of replicate experiments for α-pinene (n = 4) and β-pinene (n = 5).

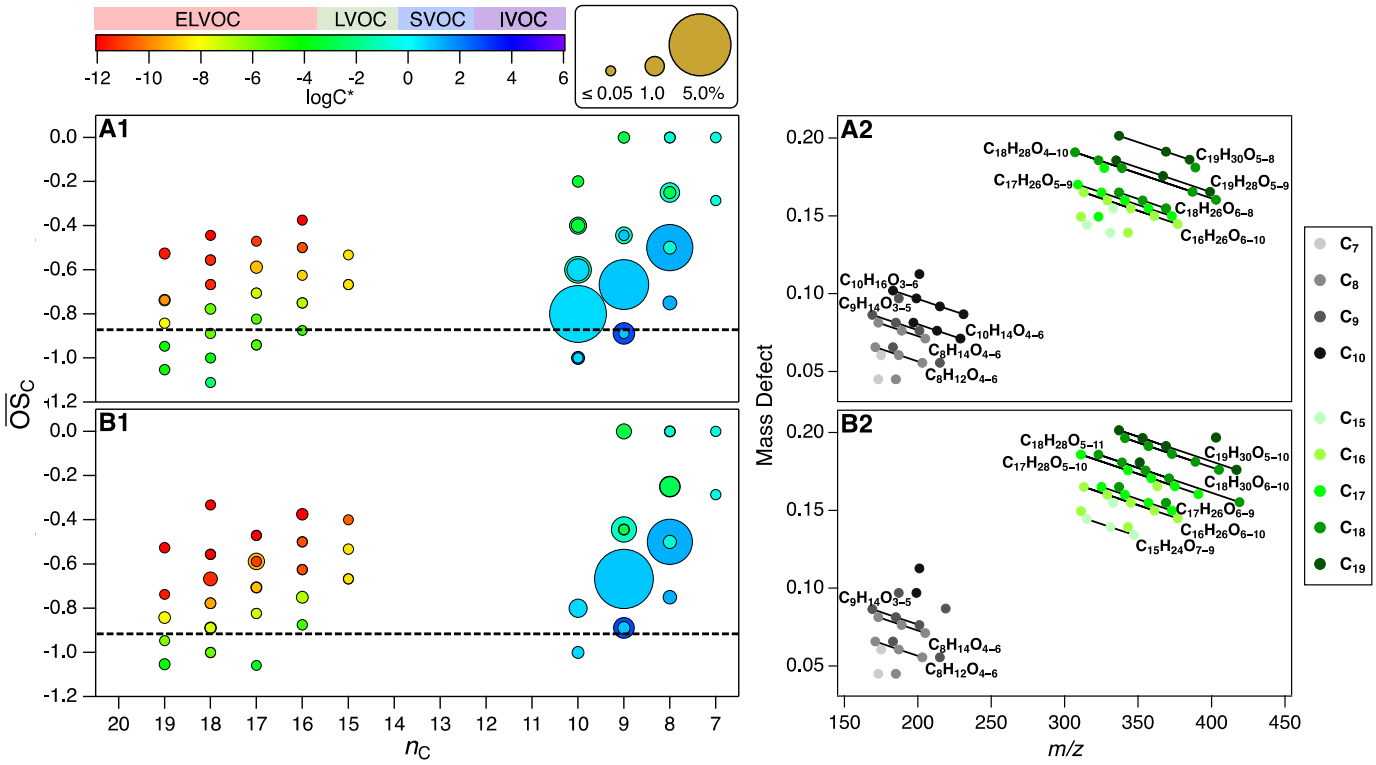

Figure 4. Molecular products identified in SOA produced from ozonolysis of (A) α-pinene and (B) β-pinene mapped onto (1) the $\overline{OS}_C$-n_C space and (2) mass defect plots. Markers in (1) and (2) represent all isomers identified for a given molecular formula (Table S3). Marker size in (1) denotes total isomer mass fraction and dashed lines represent AMS-derived bulk $\overline{OS}_C$ values (Table 1), both calculated for suspended SOA after ~5 h of ozonolysis in the CTEC (see Figure 1) and reported as averages of replicate experiments for α-pinene (n = 4) and β-pinene (n = 5). logC* values were estimated using the empirical model of Donahue et al.[72]

TABLE OF CONTENTS (TOC) GRAPHIC